An Exploration of the Effects of Reversibility in Chain Transfer to Metal in Olefin Polymerization

Phillip D. Hustad,[†] Roger L. Kuhlman,*[,†] Edmund M. Carnahan,[†] Timothy T. Wenzel,[‡] and Daniel J. Arriola*[,‡]

The Dow Chemical Company, 2301 N. Brazosport Blvd., Freeport, Texas 77541, and The Dow Chemical Company, Building 1776, Midland, Michigan 48674

Received February 18, 2008; Revised Manuscript Received March 14, 2008

ABSTRACT: A kinetic model was derived to investigate the effects of reversibility in chain transfer to metal in olefin polymerization. The model predicts both number- and weight-average molecular weights, M_n and M_w, as a function of several reactor input variables including the constants for chain transfer and reversible transfer. A number of interesting and nonobvious insights into molecular weight distributions are gained from these simulations. The most revealing result is the variation of the molecular weight distribution (M_w/M_n) with conversion. In the absence of reversible transfer, the M_w/M_n is always greater than or equal to 2. Regardless of the magnitude of the reversible transfer constant, M_w/M_n approaches 2 as M_n approaches its maximum value. More dramatic deviations from $M_w/M_n = 2$ are observed for higher chain transfer constants. Polymerization data from two bis(phenoxyimine)zirconium catalyst systems are presented to demonstrate these effects. These results indicate that singular polymerizations should not be used to explore for reversible transfer characteristics, but rather a series of polymerizations should be conducted over a range of polymer conversions.

Introduction

A search of a science citation index for "olefin and polymerization and catalyst" returns more than 16 000 references from the past 16 years. This wealth of research is a tribute to the fact that polyolefins are the largest volume class of synthetic materials today, with annual production volumes exceeding 20 billion pounds worldwide. The majority of commercially available polyolefins are still produced with heterogeneous Ziegler−Natta catalysts,[1] but products from homogeneous catalysts[2] are becoming more prevalent in the marketplace. These well-defined catalysts have facilitated detailed understanding of fundamental polymerization mechanisms.[3] With this knowledge and an endless variety of possible ligand structures, catalyst chemists now have control over practically every facet of polymer microstructure, including stereochemistry,[4] comonomer content, and macromolecular branch architecture.[5] One remaining challenge is control of the distribution of comonomer within the polymer chains, "blocking" the comonomer to tailor the physical properties of the resin. Extensive efforts have been directed toward the design of systems for living olefin polymerization as one way to control comonomer distribution at a molecular level. Through a mixture of rational design and serendipity, several catalysts have been shown to exhibit controlled or living behavior by suppressing chain transfer and termination reactions.[6] These systems have enabled the production of several new types of copolymers with exciting molecular architectures. However, these catalyst systems, like other living polymerization catalysts, have an economic limitation of producing only one polymer chain per catalyst.

The molecular weight of a polyolefin generated with a nonliving catalyst is regulated by the ratio of the rate of propagation to cumulative chain termination and transfer, normally a combination of β-hydride elimination, chain transfer to monomer, and hydrogenolysis (Figure 1).[7] Transfer of polymer chains to a metal-based chain transfer agent (CTA) is another well-known mechanism for molecular weight control in olefin polymerization.[1,8−10] In special instances, this CTA actually transfers polymer chains back to the catalyst where they can undergo further growth. This process, recently called coordinative chain transfer polymerization (CCTP),[11] operates by fast exchange between "live" and "dormant" species, reminiscent of some mechanisms utilized to control free-radical polymerization processes.[12] This behavior was first observed in a single catalyst system in the early 1990s by Samsel,[13] and other CCTP systems for ethylene polymerization were summarized in a recent review.[11] More recently, Busico, Stevens, and co-workers[14] and Sita and Zhang[15] have observed CCTP behavior in propylene polymerizations. It has been observed that fast reversible chain transfer in a batch or semibatch process produces polymers with Poisson molecular weight distributions (M_w/M_n approaching 1, where M_w is the weight-average molecular weight and M_n is the number-average molecular weight), instead of the Schulz−Flory distribution ($M_w/M_n = 2$) that is ideally observed in polymerization using a single-site catalyst. For clarity and distinction from the well-known chain transfer phenomenon, we refer to these events as reversible transfer reactions and the CTA as a chain shuttling agent, or CSA. We also use the terms *irreversible chain transfer* to describe cases for which $k_{CT} > k_{RT} = 0$, *semireversible chain transfer* to describe cases in which $k_{CT} > k_{RT} > 0$, and *reversible chain transfer* when $k_{CT} \approx k_{RT} > 0$.[16]

We have recently reported two strategies that use reversible chain transfer processes to produce olefin block copolymers (OBCs) containing both hard semicrystalline and soft amorphous polyethylene segments.[17,18] One approach utilizes two catalysts that form very different copolymers in a single polymerization reactor; one catalyst has a high selectivity for ethylene while the other is capable of copolymerizing ethylene and an α-olefin.[17] The block architecture of the polymer is formed by a process that we refer to as "chain shuttling", in which chains are reversibly transferred between the catalysts via a CSA. The critical requirement of this system is that the CSA transports "live" polymer chains among active catalyst sites. This chain shuttling process produces a multiblock copolymer with non-Poisson distributions of both molecular

* Corresponding authors. E-mail: rlkuhlman@dow.com, djarriola@dow.com.
[†] TDCC, Freeport, TX.
[‡] TDCC, Midland, MI.

10.1021/ma800357n CCC: $40.75
Published on Web 05/22/2008

weight and number of blocks per chain. A second method involves conducting CCTP in a series of continuous reactors with a single catalyst.[18] This process is similar to a sequential monomer addition strategy used in living polymerization systems to form block copolymers. By changing monomer composition, the dual-reactor CCTP scheme results in chains with diblock architectures, again with non-Poisson distributions of molecular weight due to the distribution of residence times in a continuous reactor.[19]

In our search for chain shuttling behavior, we initially turned to kinetic modeling to identify some defining characteristics of reversible chain transfer. More specifically, we derived a mathematical model to investigate the effects of chain transfer reversibility on the molecular weight averages for a single-catalyst semibatch polymerization. This model was then used to investigate the effects of these chain transfer processes on the molecular weight averages (M_n and M_w) of the resulting polymers. Importantly, we find that these properties are a complex function of not only the relevant rates but also the extent of conversion of monomer to polymer. In this article, we describe the origins of this kinetic model, the sometimes surprising results of some of our simulations, and some supporting experimental evidence of this behavior.

Results

Mathematical Depiction of the Kinetics Scheme. Our approach to polymer chain growth modeling is based on population balances for the various polymer species participating in and resulting from chain growth and transfer.[20] The kinetics scheme is written below in mathematical fashion and is a precursor to the derivation of population balances. For reference, the many variables described herein and their definitions are summarized in a notation section at the end of the article. Monomer units are represented as M, and growing polymer chains are represented by the symbol P_n, where n is the number of repeat units attached to the active catalyst. Dormant polymer is represented by A_n, where n is the number of repeat units attached to the CTA. "Dead" polymer chains, which arise from chain termination events such as hydrogenation and β-hydride eliminations, are represented by D_n, where n is the number of repeat units in the free polymer chain.

propagation ($n = 0, 1, 2, ...$)

$$P_n + M \xrightarrow{k_p} P_{n+1} \qquad \text{rate} = k_p[M][P_n]$$

background chain transfer ($n = 1, 2, 3, ...$)

$$P_n \xrightarrow{k_\beta} P_0 + D_n \qquad \text{rate} = k_\beta[P_n]$$

chain transfer to virgin CTA ($n = 1, 2, 3, ...$)

$$P_n + A_0 \xrightarrow{k_{CT}} P_0 + A_n \qquad \text{rate} = k_{CT}[P_n][A_0]$$

reversible chain transfer ($n, m = 1, 2, 3, ...$)

$$P_n + A_m \xrightarrow{k_{RT}} P_m + A_n \qquad \text{rate} = k_{RT}[P_n][A_m]$$

Population balances are derived assuming ideal mass action rate laws which are independent of polymer chain size. These population balances can be viewed as an infinite set of ordinary differential equations in time since the key index, n, ranges from 1 to infinity. The population balances for macromolecular species are shown below for growing polymer (P_n), dormant polymer (A_n), and dead polymer (D_n) having n monomeric repeat units. Constant reaction volume is assumed. Similar balance equations for virgin CTA, denoted A_0, are also given.

$$\frac{d[P_n]}{dt} = k_p[M]([P_{n-1}] - [P_n]) - (k_\beta + k_{CT}[A_0] + k_{RT}\sum_{m=1}^{\infty}[A_m])[P_n] + k_{RT}\sum_{m=1}^{\infty}[P_m][A_n] \quad (1)$$

$$\frac{d[A_n]}{dt} = k_{CT}[A_0][P_n] - k_{RT}\sum_{m=1}^{\infty}[P_m][A_n] + k_{RT}\sum_{m=1}^{\infty}[A_m][P_n] \quad (2)$$

$$\frac{d[D_n]}{dt} = +k_\beta[P_n] \quad (3)$$

$$\frac{d[A_0]}{dt} = -k_{CT}\sum_{m=1}^{\infty}[P_m][A_0] \quad (4)$$

The nonmacromolecular species P_0 results from chain transfer or preinitiation. For nonliving addition polymerization, it is

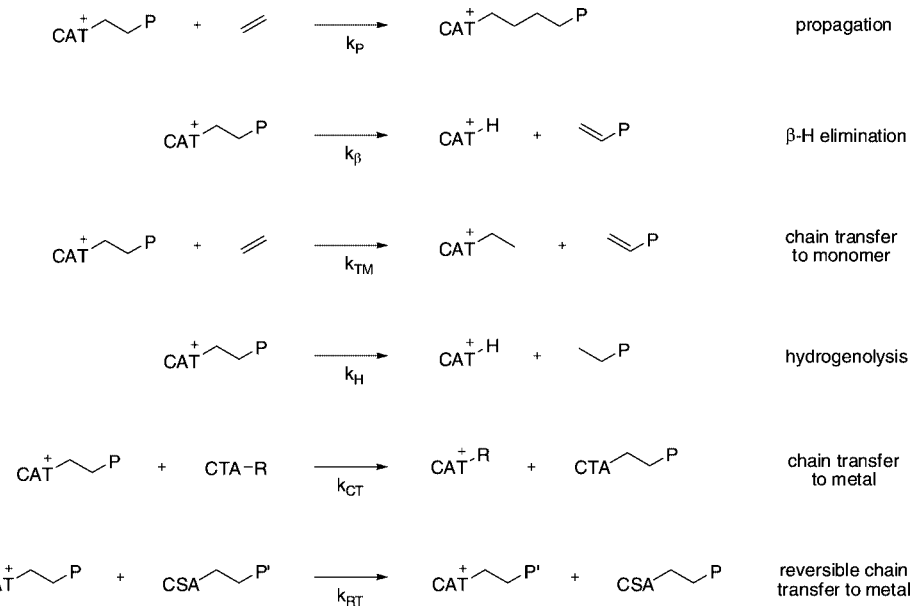

Figure 1. Propagation, transfer, and termination reactions in olefin polymerization.

Scheme 1

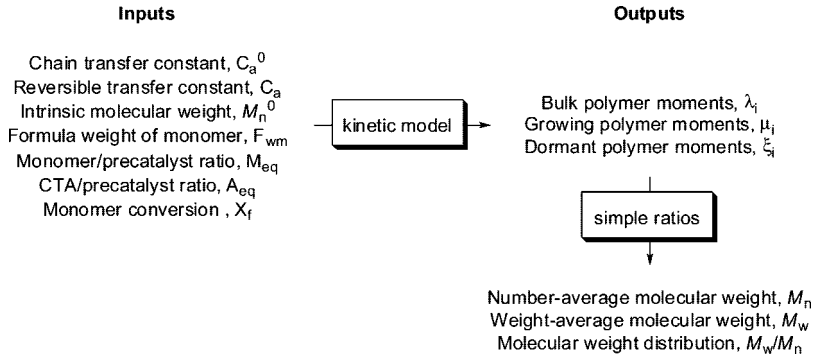

standard practice to assume that this species quickly reacts with monomer to make P_1. Such an assumption is equivalent to that of instantaneous initiation and results in a term used to solve the population balance for P_1.

$$k_p[M][P_0] \approx (k_\beta + k_{CT}[A_0])\sum_{m=1}^{\infty}[P_m] \tag{5}$$

The simplest scenario to simulate is a homopolymerization during which the monomer concentration is held constant and products are not removed, also known as a semibatch polymerization. We assume a constant reaction volume in order to simplify the system of equations. Conversion of monomer to polymer, X_f, defined as the mass ratio of polymer to free monomer, is used as an independent variable. Use of this variable simplifies the model by combining several variables, such as catalyst load, turnover frequency, and degradation rate, into a single value.[21] Also, by using conversion instead of time as an independent variable, the model only requires three dimensionless kinetics parameters. A simple balance for monomer conversion (X_f) vs time is given below, where μ_0 is the active catalyst to monomer molar ratio. This differential equation for X_f, along with the "chain rule", is used to change the independent variable from time to conversion.

$$\frac{dX_f}{dt} = k_p\sum_{m=1}^{\infty}[P_m] = k_p[M]\mu_0 \tag{6}$$

Two critical kinetics parameters give estimates of the relative rates of chain transfer and reversible transfer to propagation: the chain transfer constant for sites bearing the original alkyl moiety (virgin CTA sites), C_a^0, where $C_a^0 = k_{CT}/k_p$ and the reversible transfer constant, C_a, where $C_a = k_{RT}/k_p$. For simplicity, these simulations only consider a CTA with one transferable alkyl group. A more rigorous treatment for a CTA with multiple alkyl substituents would require more chain transfer constants (ancillary substituents may be alkyl or polymeryl), but we felt that this description was sufficient for initial investigations. The only other kinetic parameter required is the intrinsic molecular weight (M_n^0), which is used to indirectly account for background chain transfer.

Differential and algebraic equations for the moments of the molecular weight distribution (M_w/M_n) have been derived from population balances on the above kinetics scheme and are listed as eqs 5–12. In the development of the M_w/M_n model, it is assumed that reaction rates are independent of chain length, and the growing polymer population is at quasi-equilibrium with the dormant polymer. The assumption of quasi-stationary growing polymer is standard with rapid addition polymerizations such as Ziegler−Natta, metallocene, and free-radical systems. This treatment results in algebraic equations for the M_w/M_n moments for polymer species. The molecular weight moments of the polymer populations are defined in eqs 7–9 along with the conversion-domain modeling eqs 10–14. Bulk polymer in the reactor is the sum of growing, dormant, and dead chains. Separate moments are defined for bulk (λ_i), dormant (ξ_i), and growing (μ_i) polymer chain populations and nondimensionalized by division with monomer concentration, which is held constant. The zeroth moments (λ_0, ξ_0) are ratios of polymer chains concentration with monomer concentration. The first moments (λ_1, ξ_1) are ratios of repeat unit concentration with monomer concentration. Higher moments are more difficult to describe in simple terms but have been defined elsewhere.[20] These moments are dimensionless due to the use of monomer concentration ([M]) in their definition. Ratios of these moments are used to express properties such as molecular weights, with F_{wm} as the repeat unit formula weight of the monomer (e.g., 28 g/mol for ethylene).

Modeling Equations.

bulk polymer properties

$$M_n = F_{wm}\lambda_1/\lambda_0 \tag{7}$$

$$M_w = F_{wm}\lambda_2/\lambda_1 \tag{8}$$

$$M_z = F_{wm}\lambda_3/\lambda_2 \tag{9}$$

bulk polymer moments

$$\lambda_i = \frac{1}{[M]}\sum_{n=1}^{\infty} n^i([P_n] + [A_n] + [D_n]) \tag{10}$$

$$\frac{d\lambda_i}{dX_f} = \frac{C_a^0[A_0]}{[M]} + \frac{F_{wm}}{M_n^0 - F_{wm}} + \sum_{k=0}^{i-1}\binom{i}{k}\frac{\mu_k}{\mu_0} \tag{11}$$

where $$\frac{[A_0]}{[M]} = (A_{eq}/M_{eq})\exp[-C_a^0 X_f]$$

dormant polymer moments

$$\xi_i = \frac{1}{[M]}\sum_{n=1}^{\infty} n^i[A_n] \tag{12}$$

$$\frac{d\xi_i}{dX_f} = \left(\frac{C_a^0[A_0]}{[M]} + C_a\xi_0\right)\frac{\mu_i}{\mu_0} - C_a\xi_i \tag{13}$$

growing polymer moments

$$\mu_i = \frac{1}{[M]}\sum_{n=1}^{\infty} n^i[P_n] \tag{14}$$

$$\frac{\mu_i}{\mu_0} = 1 + \frac{\sum_{k=0}^{i-1}\binom{i}{k}\frac{\mu_k}{\mu_0} + C_a(\xi_i - \xi_0)}{\frac{C_a^0[A_0]}{[M]} + C_a\xi_0 + \frac{F_{wm}}{M_n^0 - F_{wm}}} \tag{15}$$

Before solution, the model must be expanded to express the individual moments of interest. The resulting algebraic and

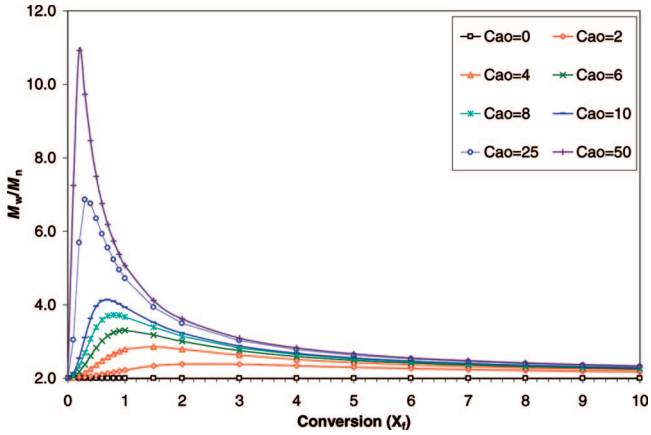

Figure 2. Simulated M_w/M_n vs conversion as a function of chain transfer constant for irreversible chain transfer, where $C_a = 0$.

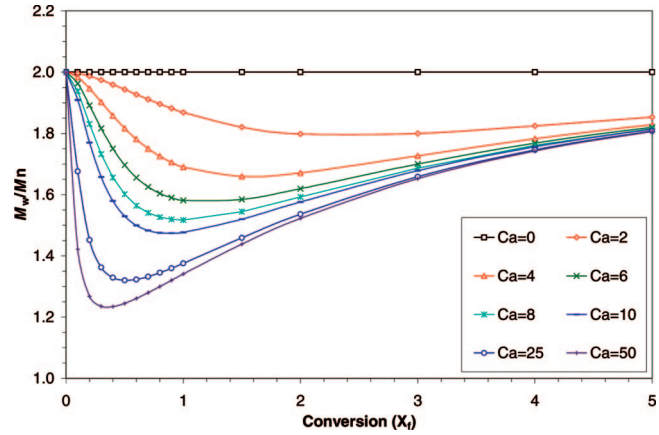

Figure 3. Simulated M_w/M_n vs conversion as a function of reversible transfer constant for reversible chain transfer, with $C_a^0 = C_a$.

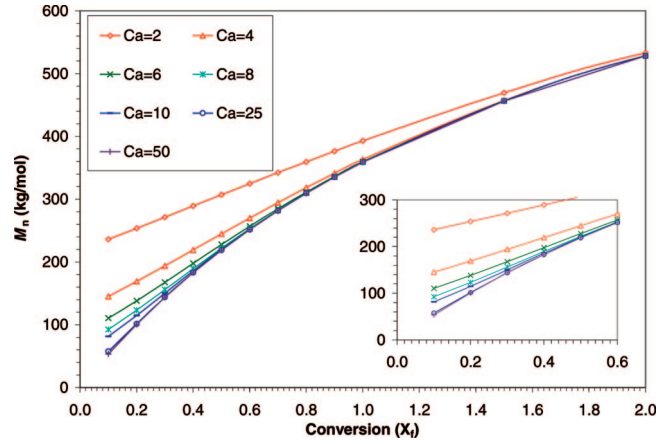

Figure 4. Simulated M_n vs conversion by reversible transfer constant for reversible chain transfer, where $C_a^0 = C_a$.

differential equations are easily solved as an initial value problem. Many aspects of the model, as well as some of the leading moments, have analytical solutions. These include the number-average molecular weight, M_n,[22] as well as the virgin CTA site concentration, $[A_0]$. The expansion and solution of the bulk polymer moments using *Mathematica* is included in the Supporting Information. It is possible with slight modifications to the *Mathematica* script to duplicate any of the simulations depicted in this report. The conversion domain model merely gives the molecular architecture as a function of conversion without regard to the time required to attain that conversion or whether that conversion is even attainable.[21] The polymerization time can be added as a model prediction by considering the differential equation $dt/dX_f = 1/(k_p[C])$, where [C] is the time-dependent concentration of active catalyst sites. Assuming a catalyst deactivation model, conversion vs time data can be used to find the value of k_p and the other rate constants.

Molecular Weight Distribution Simulations. After expansion of the model, a series of simulations was performed to investigate the effects of reaction parameters on polymer M_n and M_w/M_n. The workflow of the model, with inputs and outputs, is depicted in Scheme 1. These values depend on several variables, and fortunately, many of them are measurable or determined experimentally. These known inputs include M_n^0, which is determined by catalyst selection (and H_2 concentration); M_{eq}, the molar ratios of monomer to precatalyst, and A_{eq}, the molar ratio of CTA to precatalyst, which are determined by the experimental design; and X_f, which is directly related to the experimentally measured polymer yield. The only dependent variables are constants C_a^0 and C_a. For all the simulations described here, the intrinsic molecular weight and monomer/catalyst ratio are fixed such that $M_n^0 = 1000$ kg/mol and $M_{eq} = 1\,000\,000$, while the other inputs are varied to determine their influence on M_n and M_w.

Irreversible Chain Transfer. A number of interesting and nonobvious insights into molecular weight distributions can be gained from these simulations. For example, Figure 2 demonstrates the effect of X_f on M_w/M_n as a function of C_a^0 for irreversible chain transfer where $C_a = 0$. One can consider the horizontal axis in this plot as reaction time. Early in the reaction (i.e., low X_f), the M_w/M_n quickly rises above 2.0 due to the fast initial chain transfer, which generates a number of dead chains on the CTA with M_n much lower than M_n^0. As the reaction proceeds, the concentration of virgin CTA is depleted and normal chain transfer and termination events begin to dominate. The dead chains residing on the CTA eventually become outnumbered by eliminated chains that are "fully grown". Therefore, the M_n approaches M_n^0, and the M_w/M_n approaches 2.0 at higher X_f. The magnitude of the increase in M_w/M_n and the location of the maximum are a function of C_a^0, with higher values producing higher and earlier maximum M_w/M_n's. The M_w/M_n is greater than 2.0 at all conversions examined in the simulation for this scenario. Thus, the expected polymer from any olefin polymerization in a batch reaction with irreversible chain transfer to metal must have $M_w/M_n \geq 2$. This effect is a result of the batch nature of the reaction, in which the concentration of virgin CTA decreases to zero as conversion increases.

Reversible Chain Transfer. As an opposite extreme, cases of fully reversible chain transfer ($C_a^0 = C_a$) were simulated. The effect of conversion on M_w/M_n is plotted in Figure 3 as a function of C_a with $A_{eq} = 50$. One can consider the horizontal axis in this plot as reaction time. Early in the reaction, or low X_f, the M_w/M_n quickly plunges below 2.0, followed by a steady convergence back to 2.0 at higher X_f. Faster reversible transfer produces a lower minimum M_w/M_n and also moves this minimum to lower conversion. One interesting trend is that the M_w/M_n is less than 2.0 at all simulated conversions for reversible chain transfer with $C_a^0 = C_a$, regardless of the absolute value of C_a. This behavior sharply contrasts irreversible chain transfer, which generates polymer with $M_w/M_n \geq 2$ at all conversions.

Investigation of the effect of fully reversible chain transfer on M_n is also informative. Figure 4 depicts the relationship of M_n vs X_f as a function of C_a. As may be expected, higher chain transfer constants give lower M_n's at low conversions. In all cases, M_n increases monotonically toward M_n^0 at higher conversions. Under the model conditions used for this simulation, C_a

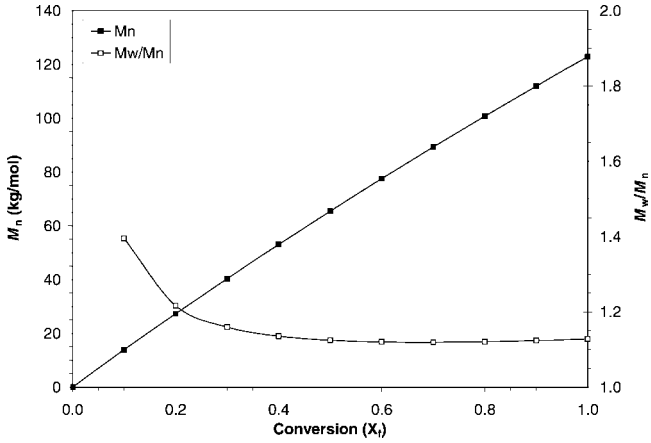

Figure 5. Simulated M_n and M_w/M_n vs conversion for polymerization with reversible chain transfer when $C_a^0 = C_a = 50$ and $A_{eq} = 200$.

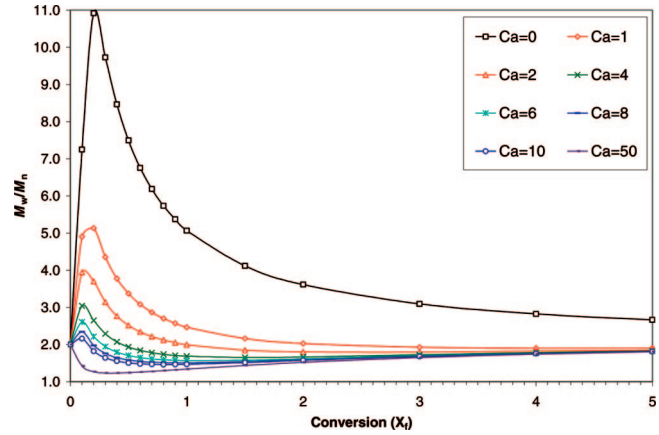

Figure 6. M_w/M_n vs conversion for semireversible chain transfer in simulations with $C_a^0 = 50$.

has very little influence on M_n for $X_f > 2$. As one might expect, plots of M_n vs X_f generally follow this pattern of monotonic increase toward M_n^0. One consequence of high C_a is the linear increase in M_n with conversion. This phenomenon, which is normally associated with a living polymerization, has been described previously for production of low molecular weight oligomers (Britovsek, G. J. P.; Cohen, S. A.; Gibson, V. C.; van Meurs, M. *J. Am. Chem. Soc.* **2004**, *126*, 10701–10712). When $C_a > 25$, the M_n increases nearly linearly up to $X_f \sim 0.5$ with a *y*-intercept near zero (see inset in Figure 4). At lower values of C_a, the near linearity extends to much higher conversions, but the apparent intercepts from linear fits of M_n for $X_f < 0.4$ increase steadily with decreasing C_a. The positive intercept reflects the competition of chain growth vs chain transfer. These trends suggest that this intercept may be a better measure of the reversible transfer rate than the goodness-of-fit for the line. In fact, these simulations indicate systems with fastest reversible transfer have the least linear plot of M_n vs yield, for a given M_n^0. However, for a plot with zero intercept, linearity should be a good indicator that M_n^0 is very high relative to the experimental range of molecular weights. At higher C_a, the initial chain transfer occurs very early in the reaction when M_n is very low. As C_a approaches zero, the ratio of rates of propagation to transfer increases, and the chains grow to higher M_n before chain transfer occurs. In the extreme of $C_a = C_a^0 = 0$ (no chain transfer to metal), M_n vs conversion is perfectly linear, with a slope of zero and apparent intercept of M_n^0.

The plot in Figure 5 depicts the response of both M_n and M_w/M_n as a function of conversion for the case of fast reversible transfer, with $C_a^0 = C_a = 50$ and $A_{eq} = 200$. At low conversion, the growth of polymer chains looks very similar to those commonly shown in publications describing "living" or "controlled" olefin polymerization. In the fast reversible chain transfer regime, these reactions bear many similarities to controlled or living free radical processes. Although many chains are growing simultaneously, only a small fraction of them are alive at any given moment, while most of the chains lie dormant on the chain transfer reagent. This behavior is also importantly not limited to the low molecular weights normally associated with catalyzed chain growth reactions, but can extend to very high molecular weight polymers if the value of M_n^0 is sufficiently high.

Each of the cases simulated above consider reactions for which the rate constants for the initial transfer from the virgin CSA and subsequent polymeryl transfer are at most equal, with $C_a^0 \geq C_a$. The magnitude of the difference in k_{CT} and k_{RT} is most likely a function of the similarities, or lack thereof, in the transferable group and the growing polymer chain. This concept is analogous to the design of living polymerization catalysts, which require the rates of initiation and propagation to be similar. If the virgin alkyl is not a good model of the growing polymer chain, initiation is likely to be slower than propagation. On the other hand, living behavior can often be realized by selecting an initiating species that closely resembles the polymer chain.

One interesting observation is revealed in an estimation of the relative rates of reversible transfer (R_{RT}) to propagation (R_P) in these systems. Since the rates are both functions of catalyst concentration, this important ratio can be estimated for the above case using M_{eq}, A_{eq}, and C_a with the following equation:

$$R_P/R_{RT} = \frac{k_p[M][P]}{k_{RT}[P][A]} = \frac{k_p[M]}{k_{RT}[A]} = \frac{[M]}{C_a[A]} \qquad (16)$$

In the above case, with $M_{eq} = 1\,000\,000$, $A_{eq} = 200$, and $C_a = 50$, the rate of propagation is 100 times faster than the rate of reversible chain transfer. Nevertheless, the simulation above clearly shows characteristics normally associated with CCTP, with a linear increase in M_n and M_w/M_n near 1.1.

Semireversible Chain Transfer. The molecular weight behavior is even more complex when the rate constants for chain transfer and shutting are inequivalent. We define this situation as semireversible chain transfer, where k_{CT} and k_{RT} are both positive, but $k_{CT} > k_{RT}$. As demonstrated in Figure 6, M_w/M_n can be greater than, less than, or equal to 2, depending on the conversion and the magnitudes of the chain transfer constants. The M_n of the polymer is simply a function of C_a^0; the value of C_a has no effect on M_n up to $C_a = C_a^0$. However, M_w is dramatically affected by lower values of C_a. If $C_a^0 \gg C_a > 0$, then the initial increase in M_w/M_n is dramatic, and M_w/M_n does not dip below 2 until high conversion. However, as C_a approaches C_a^0, the initial increase in M_w/M_n is negligible, and M_w/M_n drops below 2 at lower conversions. In any case, if $C_a > 0$, then M_w/M_n drops below but then approaches two at high conversion.[23] Early in the reaction, several chains with very low molecular weight are transferred to the CTA, similar to that observed in the previous case. However, the difference here is that these chains are not dead but are simply dormant and are eventually transferred back to the catalyst to undergo further chain growth.

Special Cases of Reversible Chain Transfer Where $C_a > C_a^0$. Just as C_a can be less than C_a^0, a reverse scenario could also be envisioned in which the initial transfer is slower than the subsequent polymeryl exchange. A likely instance of this case would be in polymerization of ethylene with an isobutyl metal complex as the CTA. The isobutyl group, with its methyl

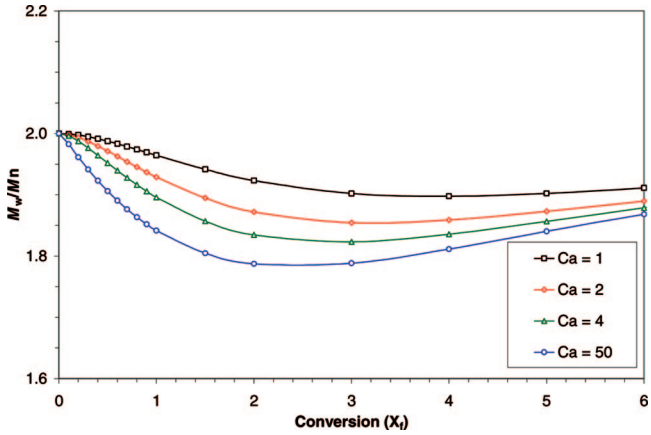

Figure 7. Simulated M_w/M_n vs conversion for a special case in which $C_a \geq C_a^0 = 1$.

branch at the β-position, is more bulky than the growing polyethylene chain and may therefore cause the initial transfer to be slower than subsequent polymeryl exchange. These cases can also be described as reversible chain transfer, but the molecular weight responses are quite different than those for which $C_a^0 > C_a$. Figure 7 demonstrates the effect of increasing C_a on the M_w/M_n as a function of conversion when $C_a^0 = 1$. The M_w/M_n is less than 2 for all investigated conversions, and the minimum M_w/M_n decreases with increasing C_a. The minimum value of M_w/M_n is both lower and occurs at lower X_f as C_a increases from 1 to 50. However, although differences clearly exist in the simulated values of M_w/M_n, it is very difficult to distinguish between these scenarios when C_a is high.

Experimental Evidence for Influence of Conversion on M_w/M_n. The kinetic model simulations described above reveal straightforward methods of determining reversibility in chain transfer. We have also observed several catalysts that display the behavior predicted by these models for reversible chain transfer. Bis(phenoxyimine) group IV complexes, originally described by Floriani[24] and later found to polymerize ethylene,[25] propylene,[26] and other α-olefins.[27] We have also found that these catalysts can be tailored to have very poor reactivity toward α-olefins and can be used in concert with copolymerization catalysts to produce OBCs through chain shuttling. Initially, we explored single catalyst/CTA combinations in a search for reversible chain transfer behavior. As described above, this can be accomplished by examining the M_n and M_w/M_n from a series of polymerizations run over a range of different conversions.

A parallel polymerization reactor[28] was used to facilitate rapid screening of several different combinations of catalysts and potential chain transfer reagents. Two representative examples that undergo fast reversible chain transfer are described below. Polymerization characteristics from ethylene/octene copolymerizations using precatalysts **1** and **2** are described in Table 1 and Table 2, and the effects of polymer yield on the molecular weight characteristics are depicted in Figure 8 and Figure 9, respectively. For each catalyst, a similar series of polymerizations across a range of conversions was performed using either Et_2Zn or bis(*tert*-butyldimethylsilyloxy)(isobutyl)aluminum (**3**). The molecular weights of polyethylenes produced by **1** and **2** in presence of **3** are insensitive to A_{eq}. Therefore, we consider the values of M_n from these experiments to be representative of M_n^0.

For catalyst **1**, the polymerizations using **3** do not show a noticeable trend of M_n or M_w/M_n across the evaluated range of yields (Figure 8a). Under these conditions, this catalyst produces fairly low molecular weight polyethylenes, with the average M_n around ~17 kg/mol and M_w/M_n around 2.4. Introduction of Et_2Zn (10 μmol) in a similar set of polymerizations induces an entirely different response (Figure 8b).The M_n increases approximately linearly up to ~7 kg/mol but then begins to level off as the M_n approaches M_n^0 at higher yields. The *y*-intercept near zero indicates that the rate of the initial transfer is fast. The M_w/M_n is also well below 2 at low yields when $M_n \ll M_n^0$ and approaches 2 as the reaction proceeds. This behavior for this catalyst/CSA pair is completely consistent with fast reversible chain transfer as predicted by the model.

A similar set of polymerizations was conducted with **2** and the same CTAs. Introduction of the bulkier 2-methylcyclohexyl moiety leads to polymers with much higher molecular weights. Again, polymerizations with **3** show no trend in molecular weight response and allow estimation of $M_n^0 \sim 260$ kg/mol (Figure 9a). Addition of 29 equiv of Et_2Zn (10 μmol) again generates a very different response. M_n increases linearly to 32 kg/mol, and M_w/M_n is below 1.4 for each sample (Figure 9b). In this case, the M_n is well below M_n^0 even at the highest yield examined, and therefore the M_w/M_n remains relatively narrow. This plot of experimental data looks remarkably similar to the simulation depicted in Figure 5 for fast reversible chain transfer.

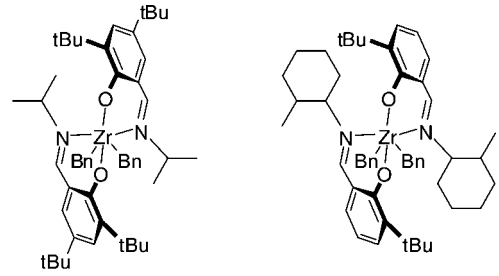

1 Bn = benzyl **2**

Conclusion

For many years, degenerative transfer mechanisms have been used to control free radical polymerizations, and these methods have enabled synthesis of various copolymer architectures. Recent work has shown that similar strategies can be applied to coordination polymerization of olefins. Using reversible chain transfer to metal alkyl reagents, we have demonstrated two strategies for synthesis of olefin block copolymers. We provide here a computational method to predict the effects of chain transfer reversibility on molecular weight behavior of olefin polymerization catalysts.

While it is very difficult to provide any "back of the envelope" methods for predicting M_w/M_n, a few general trends concerning the effects of chain transfer can be gleaned from these semibatch simulations. In all cases, M_w/M_n approaches 2 and M_n approaches M_n^0 as conversion (polymer/monomer) increases. If $M_w/M_n < 2$ at any conversion, then the chain transfer must be reversible ($C_a > 0$). Conversely, if $M_w/M_n \geq 2$ at all conversions, then chain transfer can be considered irreversible ($C_a \sim 0$). Fast, reversible chain transfer can generate a linear relationship of M_n with respect to X_f, but the line levels off as M_n approaches M_n^0. A better indicator of fast reversible transfer is an intercept near zero, while linearity implies high intrinsic molecular weight for the catalyst. The molecular weight values obtained from these simulations are clearly quite sensitive to the ratio of chain transfer reagent to monomer; increasing A_{eq} or decreasing M_{eq} has a similar effect on the evolution of molecular weights. Regardless of reversibility, more dramatic deviations from $M_w/M_n = 2$ are observed for higher C_a, higher A_{eq}, and/or lower M_{eq}. In other words, faster rates of reversible transfer relative to propagation result in lower values of M_w/M_n.

Perhaps the most noteworthy observation from these simulations is the dramatic effect of conversion of monomer to polymer

Table 1. Effect of Et_2Zn on the Molecular Weight Behavior of 1 as a Function of Conversion[a]

sample	catalyst (μmol)	Et_2Zn (μmol)	time (s)	yield (g)	M_n[c] (kg/mol)	M_w[c] (kg/mol)	M_w/M_n[c]
1[b]	0.1	0	23	0.052	14.5	34.8	2.41
2[b]	0.1	0	44	0.079	15.1	38.9	2.58
3[b]	0.1	0	86	0.104	13.7	38.9	2.84
4[b]	0.1	0	107	0.138	18.4	40.4	2.19
5[b]	0.1	0	262	0.191	16.8	42.7	2.54
6[b]	0.1	0	398	0.236	21.2	42.3	1.99
7	0.25	10	19	0.056	2.87	3.89	1.35
8	0.25	10	38	0.083	4.23	6.15	1.46
9	0.25	10	64	0.111	5.61	8.34	1.49
10	0.25	10	95	0.138	6.55	10.4	1.59
11	0.25	10	134	0.188	8.14	13.3	1.63
12	0.25	10	190	0.265	8.45	16.8	1.98

[a] General polymerization conditions: pressure = 100 psi, T = 120 °C. [b] 1 μmol of **3** used as scavenger. [c] Determined using GPC relative to polystyrene standards and converted to polyethylene equivalents.

Table 2. Effect of Et_2Zn on the Molecular Weight Behavior of 2 as a Function of Conversion[a]

sample	catalyst (μmol)	Et_2Zn (μmol)	time (s)	yield (g)	M_n[c] (kg/mol)	M_w[c] (kg/mol)	M_w/M_n[c]
13[b]	0.35	0	36	0.050	262	461	1.76
14[b]	0.35	0	1201	0.077	312	908	2.91
15[b]	0.35	0	83	0.078	222	529	2.38
16[b]	0.35	0	176	0.096	218	588	2.70
17[b]	0.35	0	1201	0.160	281	688	2.45
18	0.35	10	16	0.059	6.48	8.91	1.38
19	0.35	10	36	0.085	9.59	12.4	1.29
20	0.35	10	58	0.117	13.2	16.6	1.26
21	0.35	10	92	0.142	17.4	21.4	1.23
22	0.35	10	146	0.192	23.7	29.2	1.23
23	0.35	10	227	0.275	32.2	41.0	1.27

[a] General polymerization conditions: ethylene pressure = 100 psi, T = 120 °C. [b] 10 μmol of **3** used as scavenger. [c] Determined using GPC relative to polystyrene standards and converted to polyethylene equivalents.

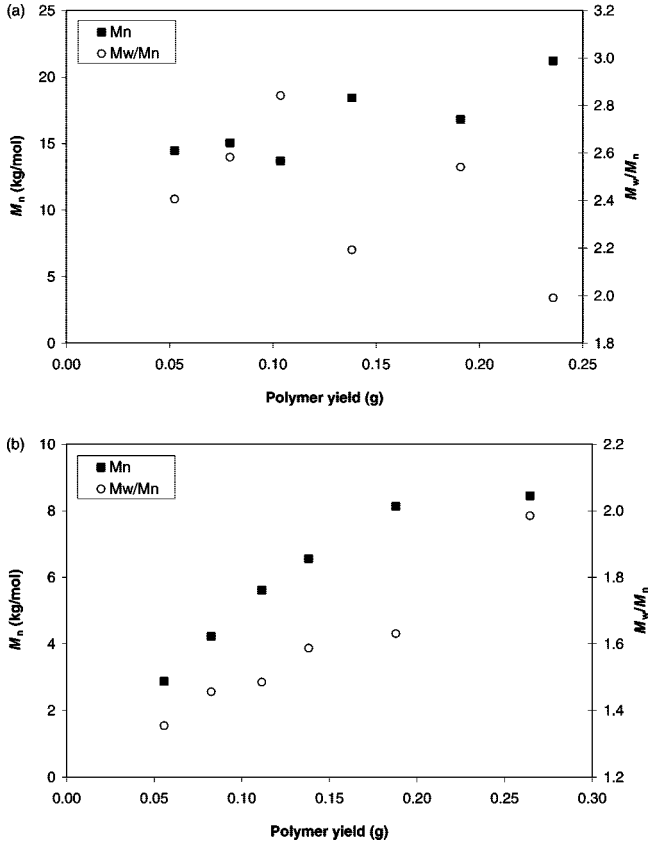

Figure 8. Effect of potential chain transfer agents on the M_w/M_n of polyethylene prepared with **1**: (a) no CTA and (b) Et_2Zn used as CTA.

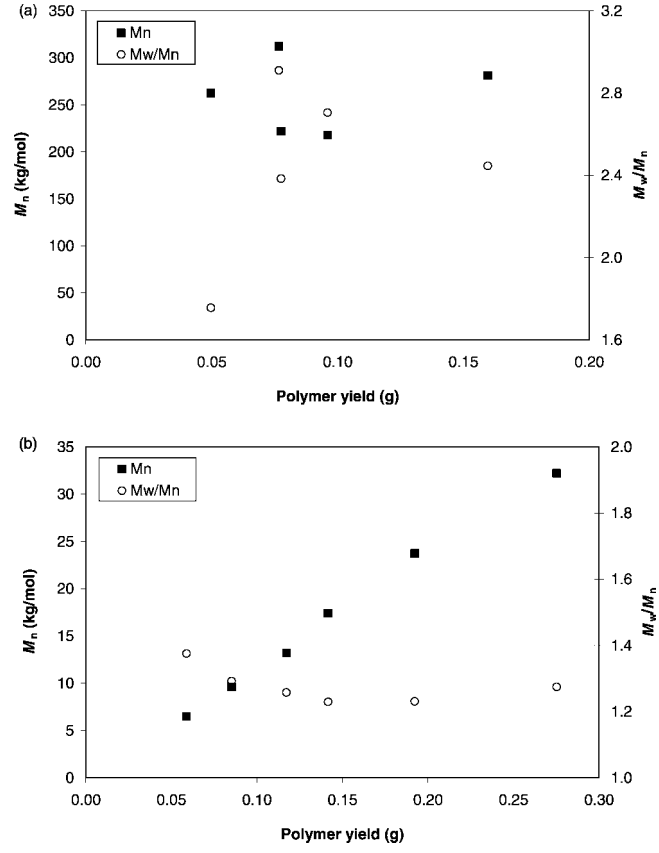

Figure 9. Effect of potential chain transfer agents on the M_w/M_n of polyethylene prepared with **2**: (a) no CTA and (b) Et_2Zn used as CTA.

on the molecular weight distribution. Any value for M_w/M_n > 1 appears to be possible using a single catalyst with a CTA in a batch reactor. To our knowledge, this is the first time this effect has been discussed in the literature. This revelation demonstrates the difficulty in determining the extent of reversibility with a particular catalyst/CTA pair. If one were to perform

only one polymerization experiment at high conversion, this behavior might easily be missed. In order to fully appreciate the reversibility in the reaction, a series of polymerizations must be conducted over a wide conversion range.

Although the molecular weight distributions are sometimes broad in these simulations, we have not observed bimodal molecular weight distributions in any simulation. In fact, there is no reason to suspect that multimodal distributions can ever be obtained by chain transfer phenomena when using a single-site catalyst. When observed, multimodal distributions are generally due to multiple catalyst sites or grossly inhomogeneous reactor conditions.

The model reported herein is relatively simple. A more thorough treatment could consider multiple valency for the CTA, Markovian, and ancillary CTA substituent effects on transfer rates and multiple catalyst types. Nonetheless, this model is sufficient to demonstrate some of the remarkable influences that chain transfer and reversible transfer can have on molecular weights and molecular weight distributions. This powerful combination of kinetic modeling and catalyst screening ultimately led to the discovery of suitable catalyst/CSA combinations for two of our methods for synthesis of OBCs. We are currently working to expand our kinetic modeling capabilities and continue to explore reversibility in chain transfer in other polymerization systems.

Experimental Section

Materials. All reagents were handled using standard procedures for air- and water-sensitive materials. Solvents and monomers were dried and deoxygenated prior to use. Diethylzinc was obtained from commercial sources and used as received. Precatalysts **1** and **2**[29] were prepared according to published procedures. The cocatalyst, a mixed C_{14-18} alkyldimethylammonium salt of bis(tris(pentafluorophenyl)-alumane)-2-undecylimidazolide,[30] and scavenger bis(*tert*-butyldimethylsilyloxy)(isobutyl)aluminum (**3**)[31] were prepared according to published procedures. All other chemicals were commercial materials and were used as received.

General High Throughput Parallel Polymerization Conditions. Polymerizations are conducted using a high throughput, parallel polymerization reactor (PPR) available from Symyx technologies, Inc., and operated substantially according to published procedures.[32–36] Ethylene copolymerizations are conducted at 120 °C and 100 psi with ethylene on demand using 1.2 equiv of cocatalyst. A series of polymerizations are conducted in a PPR comprising 48 individual reactor cells in a 6 × 8 array that are fitted with a preweighed glass tube. The working volume in each reactor cell is 6 mL. Each cell is temperature- and pressure-controlled with stirring provided by individual stirring paddles. The monomer gas and quench gas are plumbed directly into the PPR unit and controlled by automatic valves. Liquid reagents are robotically added to each reactor cell by syringes, and the reservoir solvent is mixed alkanes. The order of addition is mixed alkanes solvent (3.2 mL), ethylene, 1-octene, the cocatalyst, CTA, and catalyst. Polymerizations are conducted for approximately 1−20 min, until predetermined ethylene consumptions are reached. After quenching with CO, the reactors are cooled and the glass tubes are unloaded from the reactor. The tubes are transferred to a centrifuge/vacuum drying unit and dried for 12 h at 60 °C. The tubes containing dried polymer are weighed, and the difference between this weight and the tare weight gives the net yield of polymer. Selected details of the experiments and characterization data of the resulting polymers are listed in Tables 1 and 2.

High Throughput Characterization Methods. An automated liquid-handling robot equipped with a heated needle set to 160 °C is used to add enough 1,2,4-trichlorobenzene stabilized with 300 ppm Ionol to each dried polymer sample to give a final concentration of 30 mg/mL. A small glass stir rod is placed into each tube, and the samples are heated to 160 °C for 2 h on an orbital-shaker rotating at 250 rpm. The concentrated polymer solution is then diluted to 1 mg/mL using the automated liquid-handling robot and the heated needle set to 160 °C.

A Symyx Rapid GPC system is used to measure the molecular weight data for each sample. A Gilson 350 pump set at 2.0 mL/min flow rate is used to pump helium-purged 1,2-dichlorobenzene stabilized with 300 ppm Ionol as the mobile phase through three Plgel 10 μm (μm) Mixed B 300 mm × 7.5 mm columns placed in series and heated to 160 °C. A Polymer Laboratories ELS 1000 detector is used with the evaporator set to 250 °C, the nebulizer set to 165 °C, and the nitrogen flow rate set to 1.8 SLM (standard L/min) at a pressure of 60−80 psi (400−600 kPa) N_2. The polymer samples are heated to 160 °C, and each sample injected into a 250 μL loop using the liquid-handling robot and a heated needle. Serial analysis of the polymer samples using two switched loops and overlapping injections are used. The sample data are collected and analyzed using Symyx Epoch software. Peaks are manually integrated, and the molecular weight information is reported relative to a polystyrene standard calibration curve without correction.

Notation

Acronyms
CCTP = coordinative chain transfer polymerization
CTA = chain transfer agent
CSA = chain shuttling agent
OBC = Olefin block copolymer
Rate Parameters
k_β = β-elimination rate constant, 1/s
k_{TM} = chain transfer to monomer rate constant, L/(mol s)
k_H = hydrogenolysis rate constant, L/(mol s)
k_{CT} = chain transfer to metal rate constant, L/(mol s)
k_{RT} = reversible transfer rate constant, L/(mol s)
k_P = propagation rate constant, L/(mol s)
Kinetic Scheme Variables, with [ ] Denoting Concentration
M = monomer
P_n = growing polymer chain with n monomer units
P_0 = uninitiated catalyst
A_n = dormant polymer chain with n monomer units
A_0 = virgin CTA
D_n = dead polymer chain with n monomer units
n, m = number of monomer units in the chain
Polymer Moments
λ_i = bulk polymer moments as defined by eq 10
ξ_i = dormant polymer moments as defined by eq 12
μ_i = growing polymer moments as defined by eq 14
μ_0 = active catalyst to monomer molar ratio
Model Inputs
C_a^0 = chain transfer constant, k_{CT}/k_p
C_a = reversible transfer constant, k_{RT}/k_p
M_n^0 = intrinsic number-average molecular weight
F_{wm} = formula weight of the monomer
M_{eq} = monomer to precatalyst ratio
A_{eq} = CTA to precatalyst ratio
X_f = monomer conversion, or mass ratio of polymer to monomer
Model Outputs
M_n = number-average molecular weight ($F_{wm}\lambda_1/\lambda_0$)
M_w = weight-average molecular weight ($F_{wm}\lambda_2/\lambda_1$)
M_w/M_n = molecular weight distribution polydispersity ($\lambda_2\lambda_0/(\lambda_1)^2$)

Supporting Information Available: Expansion and solution of the modeling equations and tables of molecular weight as a function of conversion from the simulations. This material is available free of charge via the Internet at http://pubs.acs.org.

References and Notes

(1) Boor, J. J. *Ziegler-Natta Catalysts and Polymerizations*; Academic: New York, 1979.
(2) Gibson, V. C.; Spitzmesser, S. K. *Chem. Rev.* **2003**, *103*, 283–315.
(3) Grubbs, R. H.; Coates, G. W. *Acc. Chem. Res.* **1996**, *29*, 85–93.
(4) Coates, G. W. *Chem. Rev.* **2000**, *100*, 1223–1252.

(5) McKnight, A. L.; Waymouth, R. M. *Chem. Rev.* **1998**, *98*, 2587–2598.
(6) For reviews on living olefin polymerization, see: (a) Domski, G. J.; Rose, J. M.; Coates, G. W.; Bolig, A. D.; Brookhart, M. *Prog. Polym. Sci.* **2007**, *32*, 30–92. (b) Coates, G. W.; Hustad, P. D.; Reinartz, S. *Angew. Chem., Int. Ed* **2002**, *41*, 2236–2257.
(7) Resconi, L.; Camurati, I.; Sudmeijer, O. *Top. Catal.* **1999**, *7*, 145–163.
(8) Natta, G.; Pasquon, I. In *Advances in Catalysis and Related Subjects*; Eley, D. D., Selwood, P. W., Weisz, P. B., Eds.; Academic Press: New York, 1959; Vol. *11*, pp 1−66.
(9) Burfield, D. R. *Polymer* **1984**, *25*, 1817–1822.
(10) Kang, K. K.; Shiono, T.; Ikeda, T. *Macromolecules* **1997**, *30*, 1231–1233.
(11) Kempe, R. *Chem.−Eur. J.* **2007**, *13*, 2764–2773.
(12) For reviews on living radical polymerization, see: (a) Hawker, C. J.; Bosman, A. W.; Harth, E. *Chem. Rev* **2001**, *101*, 3661–3688. (b) Kamigaito, M.; Ando, T.; Sawamoto, M. *Chem. Rev* **2001**, *101*, 3689–3746. (c) Matyjaszewski, K.; Xia, J. H. *Chem. Rev* **2001**, *101*, 2921–2990.
(13) Samsel, E. G. Eur. Pat. 539876, **1993**.
(14) Alfano, F.; Boone, H. W.; Busico, V.; Cipullo, R.; Stevens, J. C. *Macromolecules* **2007**, *40*, 7736–7738.
(15) Zhang, W.; Sita, L. R. *J. Am. Chem. Soc.* **2008**, *130*, 442–443.
(16) If shuttling is very slow relative to propagation, a polymer blend is obtained. If shuttling is very fast relative to propagation, a random copolymer is obtained.
(17) Arriola, D. J.; Carnahan, E. M.; Hustad, P. D.; Kuhlman, R. L.; Wenzel, T. T. *Science* **2006**, *312*, 714–719.
(18) Hustad, P. D.; Kuhlman, R. L.; Arriola, D. J.; Carnahan, E. M.; Wenzel, T. T. *Macromolecules* **2007**, *40*, 7061–7064.
(19) Dotson, N. A.; Galvan, R.; Laurence, R. L.; Tirrell, M. In *Polymerization Process Modeling*; Advances in Interfacial Engineering Series; VCH Publishers: New York, 1996; p 262.
(20) Ray, W. H. *J. Macromol. Sci., Rev. Macromol. Chem.* **1972**, *C8*, 1–56.
(21) Graessley, W. W.; Uy, W. C.; Gandhi, A. *Ind. Eng. Chem. Fundam.* **1969**, *8*, 696.
(22) The Supporting Information shows a solution for M_n that is remarkably similar to that derived by Mortimer for very strong free-radical chain transfer agents. Mortimer, G. A. *J. Polym. Sci., Part A* **1972**, *10*, 163–168.
(23) This has not been rigorously proven mathematically but has always been observed in our simulations.
(24) Floriani, C.; Solari, E.; Corazza, F.; Chiesi-Villa, A.; Guastini, C. *Angew. Chem., Int. Ed. Engl.* **1989**, *28*, 64–66.
(25) Matsui, S.; Fujita, T. *Catal. Today* **2001**, *66*, 63.
(26) (a) Tian, J.; Coates, G. W. *Angew. Chem., Int. Ed.* **2000**, *39*, 3626–3629. (b) Tian, J.; Hustad, P. D.; Coates, G. W. *J. Am. Chem. Soc.* **2001**, *123*, 5134–5135. (c) Saito, J.; Mitani, M.; Mohri, J.-I.; Ishii, S.-I.; Yoshida, Y.; Matsugi, T.; Kojoh, S.-I.; Kashiwa, N.; Fujita, T. *Chem. Lett.* **2001**, 576–577.
(27) (a) Fujita, M.; Coates, G. W. *Macromolecules* **2002**, *35*, 9640–9647. (b) Hustad, P. D.; Coates, G. W. *J. Am. Chem. Soc.* **2002**, *124*, 11578–11579. (c) Saito, J.; Suzuki, Y.; Makio, H.; Tanaka, H.; Onda, M.; Fujita, T. *Macromolecules* **2006**, *39*, 4023–4031.
(28) Murphy, V.; Bei, X.; Boussie, T. R.; Brummer, O.; Diamond, G. M.; Goh, C.; Hall, K. A.; Lapointe, A. M.; Leclerc, M.; Longmire, J. M.; Shoemaker, J. A. W.; Turner, H.; Weinberg, W. H. *Chem. Rec.* **2002**, *2*, 278–289.
(29) Arriola, D. J.; Carnahan, E. M.; Cheung, Y. W.; Devore, D. D.; Graf, D. D.; Hustad, P. D.; Kuhlman, R. L.; Li Pi Shan, C.; Poon, B. C.; Roof, G. R.; Stevens, J. C.; Stirn, P. J.; Wenzel, T. T. US Pat. Appl. 2005/090427, **2005**.
(30) Lapointe, R. E. US Pat. 6395671, **1999**.
(31) Campbell, R. E., Jr.; Castille, T. G.; Chen, L.; Kilty, P. A.; Romer, D. R. WO Pat. Appl. 2006/007093, **2006**.
(32) Weinberg, W. H.; McFarland, E.; Goldwasser, I.; Boussie, T.; Turner, H.; Van Beek, J. A. M.; Murphy, V.; Powers, T. US Pat. 6248540 B1, **2001**.
(33) Weinberg, W. H.; McFarland, E.; Goldwasser, I.; Boussie, T.; Turner, H.; Van Beek, J. A. M.; Murphy, V.; Powers, T. US Pat. 6030917, **2000**.
(34) Lund, C.; Hall, K. A.; Boussie, T.; Murphy, V.; Hillhouse, G. US Pat. 6362309, **2002**.
(35) Turner, H. W.; Dales, G. C.; VanErden, L.; van Beek, J. A. M. US Pat. 6306658, **2001**.
(36) Guram, A.; Lund, C.; Turner, H. W.; Uno, T. US Pat. 6316663, **2001**.

MA800357N